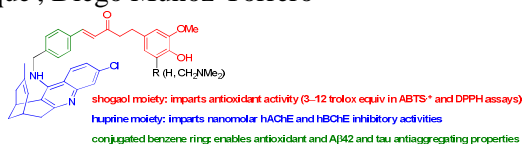# Graphical Abstract

To create your abstract, type over the instructions in the template box below.
Fonts or abstract dimensions should not be changed or altered.

Shogaol–huprine hybrids: dual antioxidant and anticholinesterase agents with β-amyloid and tau anti-aggregating properties

Leave this area blank for abstract info.

F. Javier Pérez-Areales[a], Ornella Di Pietro[a], Alba Espargaró[b], Anna Vallverdú-Queralt[c], Carles Galdeano[a], Ilaria M. Ragusa[a], Elisabet Viayna[a], Catherine Guillou[d], M. Victòria Clos[e], Belén Pérez[e], Raimon Sabaté[b], Rosa M. Lamuela-Raventós[c], F. Javier Luque[f], Diego Muñoz-Torrero[a,*]

shogaol moiety: imparts antioxidant activity (3–12 trolox equiv in ABTS⁺ and DPPH assays)

huprine moiety: imparts nanomolar hAChE and hBChE inhibitory activities

conjugated benzene ring: enables antioxidant and Aβ42 and tau antiaggregating properties

Shogaol–huprine hybrids: dual antioxidant and anticholinesterase agents with β-amyloid and tau anti-aggregating properties

F. Javier Pérez-Areales[a], Ornella Di Pietro[a], Alba Espargaró[b], Anna Vallverdú-Queralt[c], Carles Galdeano[a], Ilaria M. Ragusa[a], Elisabet Viayna[a], Catherine Guillou[d], M. Victòria Clos[e], Belén Pérez[e], Raimon Sabaté[b], Rosa M. Lamuela-Raventós[c], F. Javier Luque[f], Diego Muñoz-Torrero[a,*1]

[a] Laboratori de Química Farmacèutica (Unitat Associada al CSIC), Facultat de Farmàcia, and Institut de Biomedicina (IBUB), Universitat de Barcelona, Av. Joan XXIII, 27-31, E-08028, Barcelona, Spain

[b] Departament de Fisicoquímica, Facultat de Farmàcia, and Institut de Nanociència i Nanotecnologia (IN²UB), Universitat de Barcelona, Av. Joan XXIII, 27-31, E-08028, Barcelona, Spain

[c] Nutrition and Food Science Department, XaRTA, INSA, Facultat de Farmàcia, Universitat de Barcelona, Av. Joan XXIII, 27-31, E-08028, Barcelona, Spain, and CIBER CB06/03 Fisiopatología de la Obesidad y la Nutrición (CIBEROBN), Instituto de Salud Carlos III, Spain

[d] Centre de Recherche de Gif, Institut de Chimie des Substances Naturelles, CNRS, LabEx LERMIT, 1, Avenue de la Terrasse, 91198 Gyf-sur-Yvette, France

[e] Departament de Farmacologia, de Terapèutica i de Toxicologia, Institut de Neurociències, Universitat Autònoma de Barcelona, E-08193, Bellaterra, Barcelona, Spain

[f] Departament de Fisicoquímica, Facultat de Farmàcia (Campus Torribera), and IBUB, Universitat de Barcelona, Prat de la Riba 171, E-08921, Santa Coloma de Gramenet, Spain

ARTICLE INFO

ABSTRACT

Multitarget compounds are increasingly being pursued for the effective treatment of complex diseases. Herein, we describe the design and synthesis of a novel class of shogaol–huprine hybrids, purported to hit several key targets involved in Alzheimer's disease. The hybrids have been tested *in vitro* for their inhibitory activity against human acetylcholinesterase and butyrylcholinesterase and antioxidant activity (ABTS$^{.+}$, DPPH and Folin-Ciocalteu assays), and in intact *Escherichia coli* cells for their Aβ42 and tau anti-aggregating activity. Also, their brain penetration has been assessed (PAMPA-BBB assay). Even though the hybrids are not as potent AChE inhibitors or antioxidant agents as the parent huprine Y and [4]-shogaol, respectively, they still exhibit very potent anticholinesterase and antioxidant activities and are much more potent Aβ42 and tau anti-aggregating agents than the parent compounds. Overall, the shogaol–huprine hybrids emerge as interesting brain permeable multitarget anti-Alzheimer leads.

1. Introduction

The inexorable trend towards ageing population and increasingly higher prevalence and mortality associated with Alzheimer's disease (AD) makes more urgent than ever the development of effective treatments that address the underlying disease mechanisms. Overproduction and aggregation of β-amyloid peptide (Aβ),[1,2] hyperphosphorylation and aggregation of tau protein,[3] and oxidative stress[4,5] have been separately reported as the earliest causative factors of AD, giving rise to alternative pathological hypotheses and the derived single-target therapeutic approaches. Indeed, apart from the prevailing amyloid cascade hypothesis of AD, which posits Aβ as the main culprit of the disease,[1,2] in the past years particular emphasis has been placed on oxidative stress as a factor preceding Aβ and tau

pathologies and precipitating the pathogenesis of AD.[4–7] This has prompted the clinical study of dietary antioxidants for preventing or delaying the progression of AD.[6,7] Disappointingly, like in the case of Aβ-directed drug candidates the clinical testing of antioxidants has met with very limited success.[6,7] Even though a low bioavailability of antioxidants has been suggested as a possible reason of failure in clinical trials, their lack of clinical efficacy has been also ascribed to the fact that oxidative stress may not be the sole cause of AD,[8,9] as it would be also the case of Aβ and tau pathologies.[10] Conversely, all these processes likely display a similarly important role in a complex pathological network, making their simultaneous modulation necessary, i.e. a multitarget therapeutic intervention, in the pursuit of effective anti-Alzheimer treatments.[8,9]

*1 Corresponding autor. Tel.: +34-934024533.
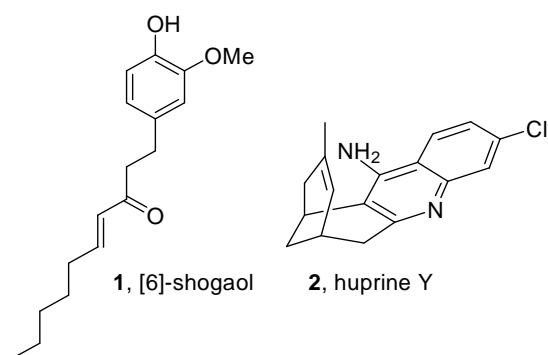*E-mail address*: dmunoztorrero@ub.edu (D. Muñoz-Torrero).

Figure 1. Structures of the natural antioxidant [6]-shogaol and the AChE inhibitor huprine Y.

In the past years intensive research efforts have been made for developing multitarget anti-Alzheimer hybrid compounds that hit several of these processes, prominently Aβ aggregation and oxidative stress, as well as the cholinergic deficit responsible for the cognitive decline of AD patients through inhibition of acetylcholinesterase (AChE).[8] Usually, the starting point for the design of such compounds is the structure of a known AChE inhibitor, which is linked to an antioxidant pharmacophoric moiety,[11–18] e.g. phenolics and polyphenolics derived fragments. The resulting hybrid compounds are in some cases endowed with Aβ antiaggregating activity, likely due to the presence of flat aromatic systems in their structures. Of note, in line with the increasingly accepted notion that the aggregation of amyloidogenic proteins, such as Aβ and tau, might share common mechanisms and might be tackled by the same drugs,[19] we have recently reported that several AChE inhibitor (huprine or tacrine)-based hybrid compounds display a dual Aβ and tau antiaggregating action, hereby broadening their multitarget profile.[20,21]

[6]-Shogaol (**1**, Fig. 1) is one of the major bioactive constituents of ginger (*Zingiber officinale*), a plant used worldwide as a spice and also widely used in the Chinese traditional medicine. It has been recently reported that [6]-shogaol exhibits potent antioxidant and anti-inflammatory activities, its enone moiety being essential for these activities.[22,23] Interestingly, [6]-shogaol enhances antioxidant defense mechanisms both in cell cultures and in mice[24] and counteracts the hydrogen peroxide-induced increase of reactive oxygen species (ROS) in HT22 cells, an *in vitro* model of hippocampal cholinergic neurons.[25]

Herein, we describe the design, synthesis, and pharmacological evaluation of a short series of multitarget anti-Alzheimer hybrid compounds that combine a unit of the highly potent AChE inhibitor huprine Y (**2**, Fig. 1) with the 4-hydroxy-3-methoxyphenylpentenone moiety of shogaols. The pharmacological characterization of these compounds includes the evaluation of their inhibitory activities towards human AChE and butyrylcholinesterase (BChE), Aβ42 and tau aggregation, and their antioxidant activity, measured through the ABTS$^{.+}$, DPPH and Folin-Ciocalteu methods. Also, the brain permeability of the novel compounds has been assessed by the widely used parallel artificial membrane permeability assay (PAMPA-BBB).

2. Results and discussion

2.1. Binding mode within human AChE: Molecular modelling studies

The antioxidant activity of shogaols seems to reside in the α,β-unsaturated ketone, apart from the phenolic ring, irrespective of the alkyl chain length.[22] Thus, for the design of the novel shogaol–huprine hybrids, the selection of the optimal length of the tether, which was to link the phenolic ring of the shogaol unit and the huprine moiety, was carried out by investigating the binding mode of the hybrids within AChE. To this end, docking calculations were performed using three models of the human AChE (hAChE), which differ in the orientation of Trp286 in the peripheral anionic site (PAS) (see section 4.3). Thus, in each model Trp286 was arranged to reflect one of the three major conformations found upon inspection of the available X-ray crystallographic structures.[26]

A series of hybrids differing in the number of methylene units present between the huprine and shogaol units were docked in the hAChE models. On the basis of docking calculations, a preferential binding to the hAChE model in which Trp286 retains the orientation found in the AChE–propidium complex (PDB ID 1N5R) in conjunction with a chain of eight carbon atoms for the tether in the shogaol–huprine hybrids (i.e. compound **5** in Scheme 1) was found. This chain length should enable the simultaneous binding to both the catalytic anionic site (CAS) and PAS of hAChE, which are at the bottom and at the entrance of the enzyme catalytic gorge, separated by a distance of approximately 14 Å.[27] Thus, the huprine unit was located in the pocket defined by residues Trp86 and Tyr337 in the CAS, forming a direct hydrogen-bond contact with the carbonyl oxygen of His447. In fact, the binding mode reproduces the main features of the arrangement found for (–)-huprine X, the 9-ethyl-analogue of huprine Y, bound to the *Torpedo californica* AChE (PDB entry 1E66),[28] and for (–)-huprine W, which bears a hydroxyethyl group at position 9, bound to the human enzyme (PDB entry 4BDT).[29] On the other hand, the phenolic ring stacked against Trp286 in the PAS (Fig. 2). Nevertheless, the flexibility conferred by the polymethylene linker in hybrid **5** leads to different arrangements of the tether in the midgorge region, because the carbonyl group present in the tether is capable of forming hydrogen bonds with either Tyr124 or Tyr72, as shown in Fig. 2A.

As the introduction of aromatic rings in the linker of dual binding site AChE inhibitors has been studied with the main aims of imposing rigidity[30] and providing additional interactions with aromatic midgorge residues, thereby increasing the inhibitory potency,[31] we also explored the potential effect of introducing a benzene ring conjugated with the α,β-unsaturated ketone (i.e. compound **9** in Scheme 2). This structural change did not alter the ability of the compound to stack against Trp86 and Trp286 in the CAS and PAS, respectively (Fig. 2B). In contrast to **5**, however, most of the docked poses clustered into a single orientation characterized by a hydrogen bond of the carbonyl unit and Tyr72. Overall, the introduction of the benzene ring conjugated with the enone does not appear to be detrimental for the binding mode of the compound within AChE, while it might be valuable to improve the pharmacological profile of the shogaol–huprine hybrids by targeting the amyloid (Aβ42 and tau) aggregation besides cholinesterase and radical scavenging activities.

2.2. Synthesis of the shogaol–huprine hybrids

First, we envisioned the synthesis of hybrid **5** (Scheme 1), bearing the 1-(4-hydroxy-3-methoxyphenyl)-4-alken-3-one moiety of shogaols, with the aliphatic chain attached to the exocyclic amino group of huprine Y.
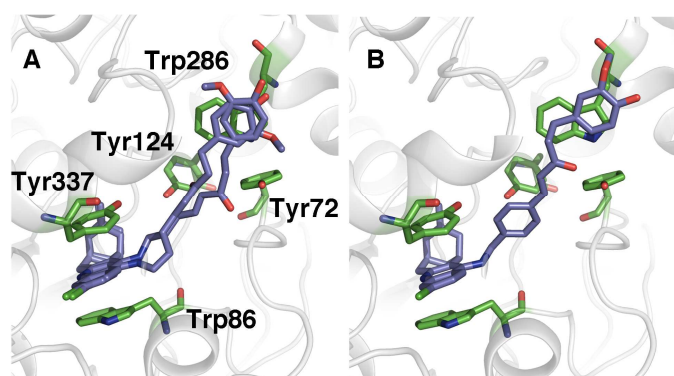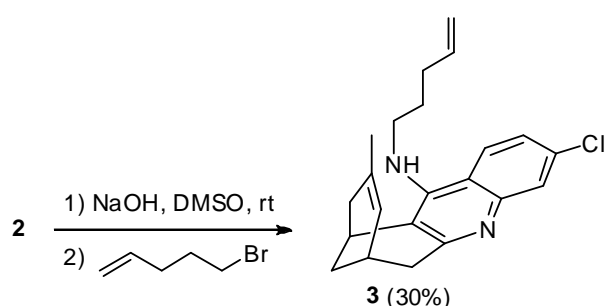
Figure 2. Structural detail of the binding mode of the shogaol–huprine hybrids **5** (A) and **9** (B) to hAChE.

Scheme 1. Synthesis of the shogaol–huprine hybrid **5**.

The synthesis of hybrid **5** involved the initial alkylation of racemic huprine Y with 5-bromo-1-pentene, which proceeded in 30% yield (Scheme 1). Subsequent cross metathesis reaction between the alkenylhuprine **3** and the known enone **4** ([4]-shogaol)[32] using the Hoveyda-Grubbs second generation catalyst in the presence of *p*-benzoquinone, afforded hybrid **5** in 15% yield, after two consecutive tedious silica gel column chromatography purifications. The observation in the ^{1}H NMR spectrum of **5** of a coupling constant of 15.6 Hz in the signals of the two enone olefin protons was clearly indicative of the *E* configuration of its carbon-carbon double bond.
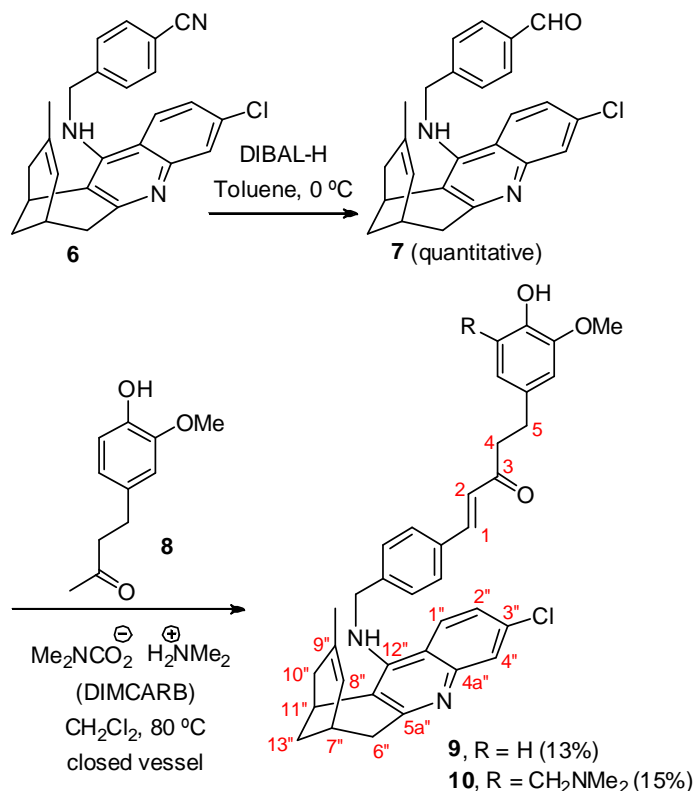
Scheme 2. Synthesis of the shogaol–huprine hybrids **9** and **10**.

For the synthesis of hybrid **9** we used as starting material the nitrile **6**,[20] which was quantitatively reduced with DIBAL-H to the corresponding aldehyde, **7** (Scheme 2). Next, we carried out a Mannich-type condensation of aldehyde **7** with zingerone, **8**, at 80 °C in a closed vessel, promoted by dimethylammonium dimethyl carbamate (DIMCARB) through formation of the iminium cation intermediate.[32] After three consecutive silica gel column chromatography purifications of the resulting reaction crude, the desired hybrid **9** was obtained in 13% isolated yield. Of note, byproduct **10**, bearing a dimethylaminomethyl substituent at position 3 of the phenolic ring, was also isolated in 15% yield. The structure of **10** was unambiguously assigned on the basis of bidimensional NMR experiments (COSY ^{1}H/^{1}H and COSY ^{1}H/^{13}C (gHSQC or gHMBC sequences)) and HRMS.

The structural similarity of compound **10** with hybrid **9** and the fact that the presence of an aliphatic amino group in **10**, protonatable at physiological pH, might enhance the interaction of the phenolic moiety with the AChE PAS aromatic residues (mainly Trp286) prompted us to subject also compound **10** to biological evaluation.

2.3. Acetylcholinesterase inhibitory activity

The inhibitory activity of the racemic shogaol–huprine hybrids **5**, **9**, and **10** against recombinant hAChE was evaluated by the method of Ellman *et al.*,[33] and compared with that of the parent racemic huprine Y, **2**, and [4]-shogaol, **4**, under the same assay conditions.

Table 1
Inhibitory activities of shogaol–huprine hybrids and reference compounds against AChE, BChE, Aβ42 and tau aggregation, antioxidant capacity, and BBB predicted permeabilities

Compd	hAChE IC$_{50}$ (nM)[a]	hBChE IC$_{50}$ (nM)[a]	ABTS$^{.+}$ (trolox equiv.)[b]	DPPH (trolox equiv.)[b]	Total phenolics (mg gallic acid equiv / g sample)[b]	Aβ42 aggregation (% inhib. at 10 µM)[c]	Tau aggregation (% inhib. at 10 µM)[c]	Pe (10^{-6} cm s^{-6})[d] (Prediction)
5	6.7 ± 0.1	982 ± 190	7.6 ± 0.6	6.6 ± 0.5	29.8 ± 2.6	39.3 ± 2.8	35.2 ± 2.3	11.7 ± 0.4 (CNS+)
9	18.3 ± 2.0	742 ± 74	10.5 ± 0.6	8.8 ± 0.7	50.0 ± 2.4	70.6 ± 4.3	51.0 ± 1.9	6.5 ± 0.8 (CNS+)
10	21.1 ± 1.9	181 ± 27	11.8 ± 0.5	2.8 ± 0.1	68.8 ± 4.3	53.9 ± 4.4	40.1 ± 2.4	8.4 ± 1.3 (CNS+)
2	0.7 ± 0.03[e]	175 ± 6[e]	2.6 ± 0.2	1.0 ± 0.01	10.2 ± 1.3	8.9 ± 1.3	7.6 ± 3.4	21.9 ± 1.2 (CNS+)
4	[f]	[g]	26.2 ± 0.2	12.2 ± 0.2	384 ± 25	10.5 ± 0.8	9.2 ± 0.7	14.7 ± 0.5 (CNS+)
Gallic acid			18.6 ± 0.1	10.3 ± 0.04	1033 ± 25			

[a] IC$_{50}$ inhibitory concentration (nM) of human recombinant AChE and human serum BChE. IC$_{50}$ values are expressed as mean ± standard error of the mean (SEM) of at least four experiments, each performed in duplicate.

[b] Antioxidant capacity measured through ABTS^{+}, DPPH, or total polyphenols. Values are expressed as mean ± SEM of three experiments.

[c] % Inhibition of Aβ42 and tau protein aggregation at 10 µM in intact *E. coli* cells. Values are expressed as mean ± SEM of four independent experiments.

[d] Permeability values from the PAMPA-BBB assay. Values are expressed as the mean ± SD of three independent experiments.

[e] Data from ref. 34.

[f] 28% inhibition at 10 µM.

[g] 6% inhibition at 10 µM.

The shogaol–huprine hybrids are very potent inhibitors of hAChE, with IC$_{50}$ values in the low nanomolar range (7–21 nM), being much more potent than the parent [4]-shogaol (28% inhibition at 10 µM) but less potent than huprine Y (Table 1). The most potent hybrid was compound **5**, which is indeed the most genuine shogaol–huprine hybrid, as it formally results from merging the structure of [4]-shogaol and huprine Y. Hybrid **5** is however only 3-fold more potent than analogues **9** and **10**, bearing a benzene ring conjugated with the shogaol enone group. The presence of an additional basic nitrogen atom at the phenolic ring in hybrid **10** has no influence on the hAChE inhibitory activity, this compound being equipotent to hybrid **9** (Table 1).

2.4. Butyrylcholinesterase inhibitory activity

Like AChE, BChE hydrolyzes the neurotransmitter acetylcholine in brain. This role of BChE is especially important when the amount of AChE in CNS decreases in the advanced stages of AD. For this reason, inhibition of BChE is an increasingly pursued activity in the search for anti-Alzheimer agents.[35] In this light, the BChE inhibitory activity of the shogaol–huprine hybrids against human serum BChE (hBChE) was evaluated by the method of Ellman *et al.*.[33]

The parent huprine Y exhibits a potent hBChE inhibitory activity, even though it is much more potent against hAChE (250-fold). Conversely, the parent [4]-shogaol is essentially inactive for hBChE inhibition (6% inhibition at 10 µM). Like huprine Y, the shogaol–huprine hybrids turned out to be potent inhibitors of hBChE (submicromolar IC$_{50}$ values) and selective towards hAChE (selectivity factors of 9–147) (Table 1). The structural features leading to higher hBChE inhibitory activity were just the opposite as for hAChE inhibition, i.e. the hybrids bearing the benzene ring conjugated with the shogaol enone moiety were the most potent, and, in this case, the presence of the amino group at the phenolic ring had a significant influence on this activity, hybrid **10** being 5- and 4-fold more potent hBChE inhibitor than **5**, and **9**, respectively, and equipotent to huprine Y.

2.5. Antioxidant activity

To evaluate the putative beneficial effects of the shogaol–huprine hybrids against oxidative stress, their antioxidant capacity (AC) and that of the parent huprine Y and [4]-shogaol was assessed using an ABTS$^{.+}$ radical decolorization assay and the DPPH assay. For many years the Folin-Ciocalteu (F-C) assay has been used as a measure of total phenolics (TP) in natural products. However, because the basic mechanism is an oxidation/reduction reaction, it can be considered another method for the assessment of AC.[36] Consequently, the shogaol–huprine hybrids were also subjected to this assay. Gallic acid, a naturally occurring phenolic acid, and trolox, a water-soluble analogue of vitamin E, with well-established antioxidant activities were also evaluated as positive standards. The results were calculated as trolox equivalents (µmol trolox / µmol tested compound) for the ABTS$^{.+}$ and DPPH assays and as mg of gallic acid equivalents (GAE)/g sample for the F-C assay.

The shogaol–huprine hybrids exhibited a potent antioxidant activity in the ABTS$^{.+}$ and DPPH assays (3–12 trolox equiv., Table 1), as well as in the TP assay. The order of antioxidant potencies was **10 > 9 > 5**, with the sole exception of the DPPH assay, where hybrid **10** was surprisingly less potent than their analogues, albeit still being 3-fold more potent than trolox. As compared with the reference compounds, the hybrids were less potent antioxidant agents than the parent [4]-shogaol, **4**, and gallic acid, but more potent than huprine Y, **2**, the latter strikingly displaying a remarkable potency, especially in the ABTS$^{.+}$ and DPPH assays (1–2.6 trolox equiv.). The antioxidant activity found in this work for huprine Y might account for the neuroprotective effect recently found in another class of huprine-based heterodimeric compounds against the hydrogen peroxide insult in neuroblastoma SHSY5Y cells.[37]

Thus, even though the shogaol phenolic ring and the enone group and, to a minor extent, the huprine moiety of these hybrids must impart antioxidant activity, the presence in the linker of the benzene ring conjugated with the shogaol enone group as well as the dimethylaminomethyl group at the shogaol phenolic ring of **10** seemed to be beneficial for antioxidant activity.

Overall, the potent antioxidant activity of the shogaol–huprine hybrids constitutes a very valuable complement to their potent

anticholinesterase inhibitory activities in the context of a multitarget anti-Alzheimer treatment.

2.6. Aβ42 and tau anti-aggregating activity

Together with oxidative stress and cholinergic dysfunction, amyloid and tau pathologies are regarded as pivotal pathogenic factors in AD, and therefore, of prime importance as targets of multifunctional drugs.

Some classes of AChE inhibitors, especially dual binding site inhibitors, are often endowed with Aβ anti-aggregating properties,[38] which arise either from blockade of the AChE peripheral anionic site (PAS) (blockade of AChE-induced Aβ aggregation)[39–41] or from a direct interaction with Aβ (blockade of spontaneous Aβ aggregation), in the latter case likely due to the presence of aromatic planar moieties in the inhibitors.

Overexpression of amyloid-prone proteins in bacteria usually leads to the formation of insoluble inclusion bodies (IBs), which display the main amyloid-like features. Taking advantage of the fact that amyloid aggregation can be followed *in vivo* in bacteria, we have recently developed a methodology that allows the fast, easy, and inexpensive screening of inhibitors of the spontaneous aggregation of potentially any amyloidogenic protein that can be overexpressed in *Escherichia coli* cells.[21] When these proteins aggregate inside *E. coli* they usually form IBs that can be stained with Thioflavin-S (Th-S). The extent of aggregation of those proteins can be monitored measuring the variations of the fluorescence of Th-S. In brief, overexpression of recombinant amyloid-prone proteins entails an increase of Th-S fluorescence compared to bacteria that do not express the protein. When bacteria overexpressing recombinant amyloid-prone proteins are grown in the presence of amyloid aggregation inhibitors the Th-S fluorescence is clearly reduced. Because the Th-S fluorescence is directly proportional to the amyloid amount in bacteria, the anti-aggregating capacity of each inhibitor can be easily determined. The Th-S binding to IBs can be assessed either by steady-state fluorescence or by visualization of IBs using optical microscopy under UV-light. In the latter case, the fluorescence is determined using image processing programs. Of note, we have shown that the results obtained in the screening of inhibitors of Aβ42 aggregation correlate well with the Aβ anti-aggregating activity values found *in vitro* using synthetic Aβ42,[21] this methodology thus emerging as a economic surrogate of the classical *in vitro* tests.

The Aβ42 and tau anti-aggregating activity of the novel shogaol–huprine hybrids were determined using this methodology (Table 1 and Figs. 3 and 4). In line with previous findings with other structural families, similar potencies for each hybrid against Aβ42 and tau aggregation and the same order of potencies for both activities among the three hybrids were found, which supports the existence of common mechanisms behind the aggregation of different amyloidogenic proteins and the likelihood of common treatments against different amyloidogenic diseases.[19] In this particular class of compounds, the Aβ42 and tau anti-aggregating activities were in the ranges 39–71% and 35–51%, respectively, using a 10 μM concentration of the hybrids, they being clearly more potent than the parent huprine Y and [4]-shogaol, **4** (around 10% inhibition at 10 μM, Table 1).

The order of potencies among the hybrids for both activities was **9** > **10** > **5**. As expected, the presence of the additional benzene ring in the linker of hybrids **9** and **10** relative to **5** led to higher Aβ42 and tau anti-aggregating activities. On the other hand, the presence of the dimethylaminomethyl group in the phenolic ring of **10** was rather detrimental for these activities.
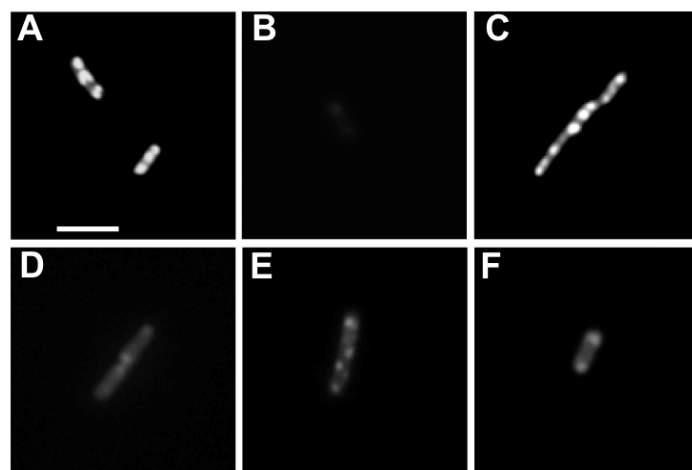

Figure 3. Optical fluorescence microscopy images under UV light of bacterial cells overexpressing Aβ42 peptide stained with Th-S. A) Induced control; B) not induced control; and in the presence of anti-aggregating compounds: C) huprine Y; D) hybrid **9**; E) Hybrid **10**; F) Hybrid **5**. Scale bar corresponds to 5 μm.
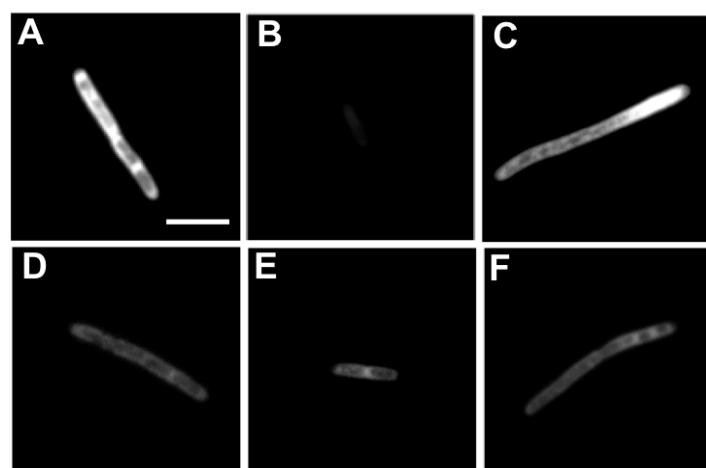

Figure 4. Optical fluorescence microscopy images under UV light of bacterial cells overexpressing tau protein stained with Th-S. A) Induced control; B) not induced control; and in the presence of anti-aggregating compounds: C) huprine Y; D) hybrid **9**; E) Hybrid **10**; F) Hybrid **5**.. Scale bar corresponds to 5 μm.

The Aβ42 and tau anti-aggregating potencies of the hybrids seem to be independent from their AChE inhibitory activities. One the one hand, the anti-aggregating potencies of the hybrids and the parent huprine Y do not correlate with their AChE inhibitory potencies. On the other hand, the Aβ42 and tau anti-aggregating potencies are determined in the absence of AChE. Even though the precise mechanisms involved in the Aβ42 and tau anti-aggregating activity of the shogaol–huprine hybrids are not known, as previously mentioned and in agreement with the beneficial effect of the additional benzene ring in hybrids **9** and **10**, the presence of several aromatic moeties with extended π-conjugated systems seems to play an important role.[42]

Overall, hybrids **9** and **10** emerge as moderately potent Aβ42 and tau anti-aggregating agents, with IC$_{50}$ values that must be in the low micromolar range.

2.7. Brain penetration

A good permeation through the blood–brain barrier (BBB) is a necessary condition for CNS drugs. Previous results from *in vitro*, *ex vivo*, and *in vivo* studies have shown that huprine Y and several classes of huprine-based hybrid compounds can readily cross the BBB, leading to central effects.[20,34,43,44] Conversely, phenolic antioxidants usually have low bioavailabilities and inherent difficulties to cross the BBB,[6,9,45] thereby making it imperative the assessment of the ability of the shogaol–huprine hybrids to enter the brain.

Brain permeation of these hybrids was determined through an *in vitro* test that uses an artificial membrane model, namely the well-established PAMPA-BBB method.[46] The *in vitro* permeability (P_e) of the shogaol–huprine hybrids, the parent compounds huprine Y and [4]-shogaol, and 14 commercial drugs, the later used for assay validation (Table 2, Experimental), through a lipid extract of porcine brain was determined. Comparison of the experimental and reported permeability values of commercial drugs provided a good linear correlation: P_e (exp) = 1.5605 P_e (lit) – 1.0507 (R^2 = 0.9308). Using this equation and the limits established by Di *et al.* for BBB permeation,[46] it was established that compounds with P_e (10^{-6} cm s^{-1}) > 5.2 would have high BBB permeation (CNS+) and compounds with P_e (10^{-6} cm s^{-1}) < 2.1 would have low BBB permeation (CNS−).

The three shogaol–huprine hybrids, like the parent huprine Y and [4]-shogaol, were predicted to be able to cross the BBB, as their P_e values were above the threshold for high BBB permeation (Table 1), which should enable them to reach their multiple CNS targets. Notwithstanding the apparent brain permeability of the shogaol–huprine hybrids, it would remain to be determined whether other pharmacokinetic properties are so favourable, especially taking into account the known phase II metabolic liability of polyphenolic compounds.[47,48]

3. Conclusion

We have synthesized the shogaol–huprine hybrids **5**, **9**, and **10** through two-step synthetic sequences starting from the known huprine Y or its *N*-(4-cyanobenzyl) derivative **6**, which involve as the key step a cross metathesis or a Mannich-type condensation reaction. In agreement with the design strategy, these hybrids turned out to be potent inhibitors of human cholinesterases (both hAChE and hBChE) and potent antioxidant agents, even though this hybridization strategy led to slightly decreased hAChE inhibitory activity relative to the parent huprine Y, as we have found in other classes of huprine-based multitarget agents,[20,34,49] or to decreased antioxidant activity relative to the parent [4]-shogaol.

The presence of the additional aromatic ring in the linker of hybrids **9** and **10**, which leads to increased antioxidant activity, seemingly enhances their interaction with Aβ42 and tau protein, leading to potent Aβ42 and tau anti-aggregating activities.

Shogaol–huprine hybrids emerge as interesting leads in the pursuit of effective treatments of AD, insofar as they might be able to readily cross the BBB and modulate several key pathological targets or events of AD such as oxidative stress, cholinergic dysfunction and Aβ and tau pathologies.

4. Experimental

4.1. Molecular modelling

Molecular modelling was performed using the X-ray crystallographic structure of hAChE (PDB ID: 4BDT).[29] The structure was refined by removal of *N*-acetyl-D-glucosamine and sulphate anions and addition of missing hydrogen atoms. Three disulfide bridges were defined between Cys residues 257–272, 409–529, and 69–96, respectively. The enzyme was modelled in its physiological active form with neutral His447 and deprotonated Glu334, which together with Ser203 form the catalytic triad. The ionization state for the rest of ionizable residues was assessed with PROPKA3.[50] Accordingly, the standard ionization state at neutral pH was considered but for residues Glu285, Glu450 and Glu452, which were protonated. Since Trp286 can adopt three main conformations in the peripheral binding site, three models were built up by re-orienting the side chain of Trp286 as found in the X-ray structures of the AChE complexes with propidium, *bis*(7)-tacrine and *syn*-TZ2PA6 (PDB ID: 1N5R, 2CKM and 1Q83, respectively).[26] These models were energy minimized using the AMBER force field.[51]

Docking of AChE inhibitors was performed using the rDock program.[52] A cavity of radius 17 Å, centered on the structure of a superligand containing huprine X, donepezil and propidium (as found in the X-ray structures 1E66, 1EVE and 1N5R) was used to define the docking volume. Since huprine X and propidium are bound to the catalytic and the peripheral binding sites, and donepezil is aligned along the gorge, this definition guarantees the exploration of the binding mode along the whole volume accessible for binding. Conformational flexibility around rotatable bonds of the ligand was allowed. Docking calculations were performed separately for the three hAChE models (see above). Conformational adjustments of other residues in the binding site were accounted for indirectly by rescaling (by a factor of 0.9) the van der Waals volume of atoms. Additionally, a pharmacophoric restraint between the protonated nitrogen in the huprine moiety of the inhibitor and the carbonyl oxygen of His447 in the CAS of the enzyme was applied. Each compound was subjected to 100 docking runs and the poses were sorted according to its docking score. The top 50 best scored poses were clustered and further analysed by visual inspection.

4.2. Chemistry

Melting points were determined in open capillary tubes with a MFB 595010M Gallenkamp melting point apparatus. 300 MHz ^{1}H, 400 MHz ^{1}H / 100.6 MHz ^{13}C and 500 MHz ^{1}H / 125.8 MHz ^{13}C NMR spectra were recorded on Varian Gemini 300, Varian Mercury 400, and Varian Inova 500 spectrometers, respectively, at the Centres Científics i Tecnològics of the University of Barcelona (CCiTUB). The chemical shifts are reported in ppm (δ scale) and coupling constants are reported in Hertz (Hz). Assignments given for the NMR spectra of hybrid **10** have been carried out on the basis of DEPT, COSY ^{1}H/^{1}H (standard procedures), and COSY ^{1}H/^{13}C (gHSQC or gHMBC sequences) experiments. IR spectra were run on a Perkin-Elmer Spectrum RX I spectrophotometer, using KBr pellets or the Attenuated Total Reflectance (ATR) technique. Absorption values are expressed as wave-numbers (cm^{-1}); only significant absorption bands are given. Column chromatography was performed on silica gel 60 AC.C (35−70 μM, SDS, ref 2000027). Thin-layer chromatography was performed with aluminum-backed sheets with silica gel 60 F$_{254}$ (Merck, ref 1.05554), and spots were visualized with UV light and 1% aqueous solution of KMnO$_4$. High resolution mass spectra of all of the new compounds were performed at the CCiTUB with a LC/MSD-TOF Agilent Technologies spectrometer. The analytical samples of all of the compounds that were subjected to pharmacological evaluation were dried at 65 ºC / 2 Torr at least for 2 days (standard conditions).

4.2.1. 3-Chloro-6,7,10,11-tetrahydro-9-methyl-12-(4-pentenyl)-7,11-methanocycloocta[b]quinoline (3)

A suspension of racemic huprine Y, **2** (1.50 g, 5.27 mmol) and finely powdered NaOH (420 mg, 10.5 mmol), and 4 Å molecular sieves in anhydrous DMSO (15 mL) was stirred, heating every 10 min approximately with a heat gun for 1 h and at rt one additional hour, and then treated dropwise with 5-bromo-1-pentene (0.69 mL, 868 mg, 5.82 mmol). The reaction mixture was stirred at rt overnight, diluted with 5N NaOH (250 mL) and extracted with EtOAc (3×300 mL). The combined organic extracts were washed with H_2O (3×200 mL), dried over anhydrous Na_2SO_4, and evaporated at reduced pressure to give a yellow oil (1.03 g), which was purified by column chromatography (35–70 µm silica gel, CH_2Cl_2/50% aq. NH_4OH 100:0.2 mixture). The alkene **3** (562 mg, 30% yield) and starting **2** (338 mg) were consecutively isolated; $R_{f(3)}$ 0.63 (CH_2Cl_2/MeOH/50% aq. NH_4OH 9:1:0.05).

A solution of **3** (106 mg, 0.30 mmol) in CH_2Cl_2 (10 mL) was filtered through a 0.2 µm PTFE filter and treated with a 0.75 N methanolic solution of HCl (1.2 mL, 0.90 mmol). The resulting solution was evaporated at reduced pressure and the solid was washed with pentane (3×2 mL) to give, after drying under standard conditions, **3**·HCl (110 mg) as a yellowish solid: mp 128–129 °C (CH_2Cl_2 / MeOH 89:11); IR (KBr) ν 3500–2500 (max at 3226, 3111, 3049, 3004, 2925, 2854, 2717, N–H, $^+$N–H, C–H st), 1717, 1699, 1684, 1669, 1629, 1582, 1569, 1560 (Ar–C–C and Ar–C–N st) cm^{-1}; ^{1}H NMR (400 MHz, CD_3OD) δ 1.57 (s, 3H, 9-CH$_3$), 1.91–2.02 (complex signal, 4H, 13-H$_{syn}$, 10-H$_{endo}$ and 2'-H$_2$), 2.08 (dm, J 12.8 Hz, 1H, 13-H$_{anti}$), 2.10 (dt, J, J' 7.2 Hz, 3'-H$_2$), 2.56 (dd, J 17.6 Hz, J' 4.8 Hz, 1H, 10-H$_{exo}$), 2.76 (m, 1H, 7-H), 2.89 (d, J 17.6 Hz, 1H, 6-H$_{endo}$), 3.21 (dd, J 17.6 Hz, J' 5.2 Hz, 1H, 6-H$_{exo}$), 3.48 (m, 1H, 11-H), 3.99 (dt, J, J' 6.8 Hz, 2H, 1'-H$_2$), 4.86 (s, NH and $^+$NH), 5.00 (ddt, J 10.4 Hz, J', J'' 1.6 Hz, 1H, 5'-H$_a$), 5.04 (ddt, J 17.2 Hz, J', J'' 1.6 Hz, 1H, 5'-H$_b$), 5.57 (br d, J 4.8 Hz, 1H, 8-H), 5.86 (ddt, J 17.2 Hz, J' 10.4, J'' 6.8 Hz, 1H, 4'-H), 7.52 (d, J 9.6 Hz, 1H, 2-H), 7.80 (s, 1H, 4-H), 8.36 (d, J 9.6 Hz, 1H, 1-H); ^{13}C NMR (100.6 MHz, CD_3OD) δ 23.5 (CH$_3$, 9-CH$_3$), 27.2 (CH, C11), 27.8 (CH, C7), 29.3 (CH$_2$, C13), 30.5 (CH$_2$), 31.9 (CH$_2$) (C2' and C3'), 36.0 (CH$_2$, C6), 36.2 (CH$_2$, C10), 50.9 (CH$_2$, C1'), 115.6 (C, C12a), 116.3 (CH$_2$, C5'), 117.9 (C, C11a), 119.1 (CH, C4), 125.1 (CH, C8), 126.6 (CH, C2), 129.4 (CH, C1), 134.5 (C, C9), 138.4 (CH, C4'), 140.1 (C, C3), 140.9 (C, C4a), 151.3 (C, C5a), 156.9 (C, C12); HRMS (ESI), calcd for [C$_{22}$H$_{25}$^{35}ClN$_2$ + H$^+$] 353.1779, found 353.1777.

4.2.2. 8-[(3-Chloro-6,7,10,11-tetrahydro-9-methyl-7,11-methanocycloocta[b]quinolin-12-yl)amino]-1-(4-hydroxy-3-methoxyphenyl)oct-4-en-3-one (5)

A mixture of a solution of alkene **3** (725 mg, 2.05 mmol) in anhydrous CH_2Cl_2 (28 mL), enone **4** (765 mg, 3.08 mmol), p-benzoquinone (21 mg, 0.19 mmol) and Hoveyda-Grubbs 2nd generation catalyst (65 mg, 0.10 mmol) was stirred under reflux for 3 days. The resulting mixture was directly purified through two consecutive column chromatographies (35–70 µm silica gel, CH_2Cl_2/MeOH/50% aq. NH_4OH and hexane/EtOAc mixtures, gradient elution), to afford hybrid **5** (158 mg, 15% yield). The analytical sample of **5** (30 mg) was obtained by preparative thin layer chromatography of an aliquot amount of the product (100 mg), followed by washing with pentane (3×3 mL); R_f 0.71 (CH_2Cl_2/MeOH/50% aq. NH_4OH 9:1:0.15); mp 69–71 °C; IR (ATR) ν 3352 (O–H, N–H st), 1666, 1660, 1632, 1603, 1572, 1556, 1514 (C=O, Ar–C–C, Ar–C–N st) cm^{-1}; ^{1}H NMR (400 MHz, $CDCl_3$) δ 1.51 (s, 3H, 9''-CH$_3$), 1.78 (br d, J 16.4 Hz, 1H, 10''-H$_{endo}$), 1.86 (tt, J, J' 6.8 Hz, 2H, 7-H$_2$), 1.92 (dm, J 12.0 Hz, 1H, 13''-H$_{syn}$), 2.05 (dm, J 12.0 Hz, 1H, 13''-H$_{anti}$), 2.33 (dtd, J, J'

6.8 Hz, J'' 1.6 Hz, 2H, 6-H$_2$), 2.54 (dm, J 16.4 Hz, 1H, 10''-H$_{exo}$), 2.74 (m, 1H, 7''-H), 2.78–2.89 (complex signal, 4H, 1-H$_2$, 2-H$_2$), 3.01 (br d, J 17.6 Hz, 1H, 6''-H$_{endo}$), 3.15 (dd, J 17.6 Hz, J' 5.2 Hz, 1H, 6''-H$_{exo}$), 3.29 (m, 1H, 11''-H), 3.46 (m, 2H, 8-H$_2$), 3.86 (s, 3H, 3'-OCH$_3$), 5.54 (br d, J 4.4 Hz, 1H, 8''-H), 6.11 (dt, J 15.6 Hz, J' 1.6 Hz, 1H, 4-H), 6.67 (dd, J 8.0 Hz, J' 2.0 Hz, 1H, 6'-H), 6.70 (d, J 2.0 Hz, 1H, 2'-H), 6.80 (dt, J 15.6 Hz, J' 6.8 Hz, 1H, 5-H), 6.82 (d, J 8.0 Hz, 1H, 5'-H), 7.27 (dd, J 8.8 Hz, J' 2.0 Hz, 1H, 2''-H), 7.87 (d, J 8.8 Hz, 1H, 1''-H), 7.89 (d, J 2.0 Hz, 1H, 4''-H); ^{13}C NMR (100.6 MHz, CD_3OD) δ 23.6 (CH$_3$), 28.4 (CH), 29.5 (CH), 30.1 (CH$_2$), 30.7 (CH$_2$), 30.8 (CH$_2$), 31.0 (CH$_2$), 38.0 (CH$_2$), 40.4 (CH$_2$), 42.8 (CH$_2$), 50.1 (CH$_2$), 56.4 (CH$_3$), 113.2 (CH), 116.1 (CH), 119.9 (C), 121.7 (CH), 122.2 (C), 125.1 (CH), 126.1 (CH), 126.6 (CH), 127.4 (CH), 131.5 (C), 131.9 (CH), 133.6 (C), 133.9 (C), 135.7 (C), 145.8 (C), 148.5 (CH), 148.9 (C), 152.8 (C), 159.4 (C), 202.4 (C); HRMS (ESI), calcd for [C$_{32}$H$_{35}$^{35}ClN$_2$O$_3$ + H$^+$] 531.2409, found 531.2405.

4.2.3. 4-{[(3-Chloro-6,7,10,11-tetrahydro-9-methyl-7,11-methanocycloocta[b]quinolin-12-yl)amino]methyl}benzaldehyde (7)

A solution of nitrile **6** (337 mg, 0.84 mmol) in anhydrous toluene (14 mL) was cooled to 0 °C and treated dropwise with DIBAL-H (1.2 M solution in toluene, 1.05 mL, 1.26 mmol). The reaction mixture was stirred at 0 °C overnight, and treated successively with 2 N HCl (5 mL) and 10 N NaOH (30 mL) at 0 °C. The resulting mixture was extracted with CH_2Cl_2 (3×50 mL) and the combined organic extracts were washed with water (2×50 mL), dried over anhydrous Na_2SO_4 and evaporated at reduced pressure to give crude aldehyde **7** (354 mg, quantitative), which was used in the next step without further purification; R_f 0.27 (CH_2Cl_2/MeOH 99:1); ^{1}H NMR (300 MHz, $CDCl_3$) δ 1.50 (s, 3H, 9'-CH$_3$), 1.72 (br d, J 17.4 Hz, 1H, 10''-H$_{endo}$), 1.85 (dm, J 12.6 Hz, 1H, 13'-H$_{syn}$), 1.98 (dm, J 12.6 Hz, 1H, 13'-H$_{anti}$), 2.46 (dm, J 17.4 Hz, 1H, 10'-H$_{exo}$), 2.73 (m, 1H, 7'-H), 3.02 (ddd, J 17.7 Hz, J', J'' 2.1 Hz, 1H, 6'-H$_{endo}$), 3.16 (dd, J 17.7 Hz, J' 5.7 Hz, 1H, 6'-H$_{exo}$), superimposed 3.14–3.20 (m, 1H, 11'-H), 4.23 (t, J 6.9 Hz, 1H, NH-CH$_2$-Ph), 4.68 (d, J 6.9 Hz, 2H, NH-CH_2-Ph), 5.53 (m, 1H, 8'-H), 7.15–7.30 (complex signal), 7.56 (d, J 8.1 Hz), and 7.80–8.00 (complex signal) [7H, 2(6)-H, 3(5)-H, 1'-H, 2'-H, 4'-H], 10.05 (s, 1H, Ph-CHO); HRMS (ESI), calcd for [C$_{25}$H$_{23}$^{35}ClN$_2$O + H$^+$] 403.1571, found 403.1578.

4.2.4. 1-{4-{[(3-Chloro-6,7,10,11-tetrahydro-9-methyl-7,11-methanocycloocta[b]quinolin-12-yl)amino]methyl}phenyl}-5-(4-hydroxy-3-methoxyphenyl)pent-1-en-3-one (9) and 1-{4-{[(3-chloro-6,7,10,11-tetrahydro-9-methyl-7,11-methanocycloocta[b]quinolin-12-yl)amino]methyl}phenyl}-5-[3-(dimethylamino)methyl-4-hydroxy-5-methoxyphenyl]pent-1-en-3-one (10)

A mixture of ketone **8** (86 mg, 0.44 mmol) in dimethylammonium dimethyl carbamate (DIMCARB, 29 µL, 30 mg, 0.23 mmol) and a solution of aldehyde **7** (178 mg, 0.44 mmol) in CH_2Cl_2 (1.2 mL) was heated in a closed vessel at 80 °C overnight and the mixture was evaporated at reduced pressure. After three consecutive purifications by column chromatography (35–70 µm silica gel, two with CH_2Cl_2/MeOH/50% aq. NH_4OH 100:0:0.2 to 99.9:0.1:0.2 and one with EtOAc as the eluents), the desired hybrid **9** (32 mg, 13% yield) and the byproduct **10** (43 mg, 15% isolated yield) were isolated; $R_{f(9)}$ 0.73 (CH_2Cl_2/MeOH/50% aq. NH_4OH 90:10:0.15); $R_{f(10)}$ 0.68 (CH_2Cl_2/MeOH/50% aq. NH_4OH 90:10:0.15).

The analytical samples of **9**·HCl (5 mg) and **10**·2HCl (27 mg) were obtained by treatment of the free bases with a 0.53 N methanolic solution of HCl (0.25 mL, 0.13 mmol for **9**; 0.45 mL,

0.24 mmol for **10**), evaporation, recrystallization from MeOH/EtOAc/hexane 1:2:0.5 (1.75 mL), and washing with pentane (3×3 mL).

9·HCl: mp 140–142 ℃ (MeOH/EtOAc/hexane 1:2:0.5); IR (ATR) ν 3500–2500 (max. at 3215, 2923, O–H, N–H, $^+$N–H, C–H st), 1631, 1600, 1582, 1563, 1513 (C=O, Ar–C–C, Ar–C–N st) cm^{-1}.

9 (free base): ^{1}H NMR (400 MHz, CDCl$_3$) δ 1.48 (s, 3H, 9"-CH$_3$), 1.70 (br d, J 16.8 Hz, 1H, 10"-H$_{endo}$), 1.83 (dm, J 12.4 Hz, 1H, 13"-H$_{syn}$), 1.97 (dm, J 12.4 Hz, 1H, 13"-H$_{anti}$), 2.43 (br dd, J 16.8 Hz, J' 3.6 Hz, 1H, 10"-H$_{exo}$), 2.72 (br s, 1H, 7"-H), 2.92–3.01 (complex signal, 4H, 4-H$_2$, 5-H$_2$), 3.02 (br d, J 17.2 Hz, 1H, 6"-H$_{endo}$), 3.148 (dd, J 17.2 Hz, J' 5.2 Hz, 1H, 6"-H$_{exo}$), superimposed 3.154 (m, 1H, 11"-H), 3.87 (s, 3H, 3'-OCH$_3$), 4.23 (br signal, 2H, OH, NH), 4.63 (br s, 2H, NH-CH_2-Ph), 5.52 (br d, J 4.4 Hz, 1H, 8"-H), 6.72 (dd, J 8.0 Hz, J' 2.0 Hz, 1H, 6'-H), 6.74 (d, J 16.4 Hz, 1H, 2-H), 6.75 (d, J 2.0 Hz, 1H, 2'-H), 6.84 (d, J 8.0 Hz, 1H, 5'-H), 7.27 (dd, J 8.8 Hz, J' 2.0 Hz, 1H, 2"-H), 7.38 (dm, J 8.0 Hz, 2H, p-phenylene-H$_{meta}$), 7.54 (d, J 8.0 Hz, 2H, p-phenylene-H$_{ortho}$), 7.55 (d, J 16.4 Hz, 1H, 1-H), 7.92 (d, J 8.8 Hz, 1H, 1"-H), 7.93 (d, J 2.0 Hz, 1H, 4"-H); ^{13}C NMR (100.6 MHz, CDCl$_3$) significant signals δ 23.3 (CH$_3$), 27.5 (CH), 28.1 (CH), 28.9 (CH$_2$), 29.7 (CH$_2$), 37.1 (CH$_2$), 39.9 (CH$_2$), 42.9 (CH$_2$), 54.0 (CH$_2$), 55.9 (CH$_3$), 111.2 (CH), 114.4 (CH), 119.1 (C), 120.8 (CH), 122.5 (C), 124.8 (CH), 125.0 (CH), 125.5 (CH), 126.4 (CH), 127.7 (CH), 128.0 (2CH), 128.8 (2CH), 141.7 (C), 141.9 (CH), 144.0 (C), 146.4 (C), 148.4 (C), 149.7 (C), 158.9 (C), 199.4 (C); HRMS (ESI), calcd for [C$_{36}$H$_{35}$^{35}ClN$_2$O$_3$ + H $^+$] 579.2409, found 579.2406.

10·2HCl: mp 163–167 ℃ (MeOH/EtOAc/hexane 1:2:0.5); IR (ATR) ν 3500–2500 (max. at 3215, 3039, 2922, 2702, O–H, N–H, $^+$N–H, C–H st), 1630, 1600, 1582, 1566, 1504 (C=O, Ar–C–C, Ar–C–N st) cm^{-1}; ^{1}H NMR (500 MHz, CD$_3$OD) δ 1.61 (s, 3H, 9"-CH$_3$), superimposed 1.95–2.00 (m, 1H, 13"-H$_{syn}$), 1.98 (br d, J 17.0 Hz, 1H, 10"-H$_{endo}$), 2.10 (dm, J 11.0 Hz, 1H, 13"-H$_{anti}$), 2.56 (dm, J 17.0 Hz, 1H, 10"-H$_{exo}$), 2.80 (m, 1H, 7"-H), 2.84 [s, 6H, 3'-CH$_2$-N(CH_3)$_2$], 2.91 (d, J 18.0 Hz, 1H, 6"-H$_{endo}$), 2.93 (t, J 7.0 Hz, 2H, 5-H$_2$), 3.07 (t, J 7.0 Hz, 2H, 4-H$_2$), 3.25 (dd, J 18.0 Hz, J' 5.5 Hz, 1H, 6"-H$_{exo}$), 3.51 (m, 1H, 11"-H), 3.89 (s, 3H, 5'-OCH$_3$), 4.27 [s, 2H, 3'-CH_2-N(CH$_3$)$_2$], 4.85 (s, OH, NH, and $^+$NH), 5.23 (s, 2H, NH-CH_2-Ph), 5.61 (dm, J 4.5 Hz, 1H, 8"-H), 6.82 (s, 1H, 2'-H), 6.88 (d, J 16.0 Hz, 1H, 2-H), 6.99 (s, 1H, 6'-H), 7.39 (dd, J 9.0 Hz, J' 2.0 Hz, 1H, 2"-H), 7.48 (br d, J 8.0 Hz, 2H, p-phenylene-H$_{meta}$), 7.65 (d, J 16.0 Hz, 1H, 1-H), 7.71 (br d, J 8.0 Hz, 2H, p-phenylene-H$_{ortho}$), 7.77 (d, J 2.0 Hz, 1H, 4"-H), 8.20 (d, J 9.0 Hz, 1H, 1"-H); ^{13}C NMR (125.8 MHz, CD$_3$OD) δ 23.5 (CH$_3$, 9"-CH$_3$), 27.6 (CH, C11"), 27.9 (CH, C7"), 29.3 (CH$_2$, C13"), 30.7 (CH$_2$, C5), 36.1 (CH$_2$, C6"), 36.3 (CH$_2$, C10"), 43.2 (CH$_2$, C4), 43.3 [2CH$_3$, 3'-CH$_2$-N(CH_3)$_2$], 52.1 (CH$_2$, NH-CH$_2$-Ph), 56.6 (CH$_3$, 5'-OCH$_3$), 57.9 [CH$_2$, 3'-CH$_2$-N(CH$_3$)$_2$], 114.7 (CH, C6'), 115.7 (C, C12a"), 117.1 (C, C3'), 118.4 (C, C11a"), 119.3 (CH, C4"), 124.3 (CH, C2'), 125.2 (CH, C8"), 126.8 (CH, C2"), 127.6 (CH, C2), 128.4 (2CH, p-phenylene-C$_{meta}$), 129.2 (CH, C1"), 130.3 (2CH, p-phenylene-C$_{ortho}$), 134.3 (C, C1'), 134.7 (C, C9"), 135.8 (C, p-phenylene-C$_{ipso}$), 140.4 (C, C3"), 140.9 (C, C4a"), 141.4 (C, p-phenylene-C$_{para}$), 143.7 (CH, C1), 145.4 (C, C4'), 149.1 (C, C5'), 152.0 (C, C5a"), 157.4 (C, C12"), 202.0 (C, C3); HRMS (ESI), calcd for [C$_{39}$H$_{42}$^{35}ClN$_3$O$_3$ + H $^+$] 636.2987, found 636.2975.

4.3. Biological profiling

4.3.1. AChE and BChE inhibitory activities

Human recombinant AChE (Sigma-Aldrich) and human serum BChE (Sigma-Aldrich) inhibitory activities were evaluated spectrophotometrically by the method of Ellman *et al.*.[33] The reactions took place in a final volume of 300 µL of 0.1 M phosphate-buffered solution pH 8.0, containing hAChE or hBChE (0.02 u/mL) and 333 µM 5,5'-dithiobis(2-nitrobenzoic) acid (DTNB; Sigma-Aldrich) solution used to produce the yellow anion of 5-thio-2-nitrobenzoic acid. Inhibition curves were performed in duplicate using at least 10 increasing concentrations of inhibitors and preincubated for 20 min at 37 ℃ before adding the substrate.[49] One duplicate sample without inhibitor was always present to yield 100% of AChE or BChE activities. Then substrates, acetylthiocholine iodide (450 µM; Sigma-Aldrich) or butyrylthiocholine iodide (300 µM; Sigma-Aldrich), were added and the reaction was developed for 5 min at 37 ℃. Colour production was measured at 414 nm using a labsystems Multiskan spectrophotometer.

Data from concentration–inhibition experiments of the inhibitors were calculated by non-linear regression analysis, using the GraphPad Prism program package (GraphPad Software; San Diego, USA), which gave estimates of the IC$_{50}$ (concentration of drug producing 50% of enzyme activity inhibition). Results are expressed as mean ± S.E.M. of at least 4 experiments performed in duplicate.

4.3.2. Antioxidant activity
4.3.2.1. Standards and reagents

Folin-Ciocalteu (F-C) reagent, sodium carbonate, ABTS (2,2'azino-bis(3-ethylbenzothiazoline-6-sulfonic acid), trolox ((±)-6-hydroxy-2,5,7,8-tetramethylchromane-2-carboxylic acid), caffeic acid, chlorogenic acid, gallic acid, quercetin, ascorbic acid, and manganese dioxide were purchased from Sigma Aldrich (Madrid, Spain), and DPPH (2,2-diphenyl-1-picrylhydrazyl) from Extrasynthèse (Genay, France). MeOH and EtOH were obtained from Scharlau (Barcelona, Spain), HOAc from Panreac (Barcelona, Spain), anhydrous sodium acetate (2 M) from Merck (Darmstadt, Germany), and ultrapure water (Milli-Q) from Millipore (Bedford, USA).

4.3.2.2. Sample pretreatment

Samples (1 mg) were weighed and homogenized with EtOH (1 mL). The homogenate was sonicated for 5 min and filtered through a 0.45 µm polytetrafluoroethylene (PTFE) filter from Waters (Milford, USA) into a vial.

4.3.2.3. Antioxidant capacity: ABTS$^{·+}$ assay

The antioxidant capacity (AC) was first measured using an ABTS$^{·+}$ radical decolorization assay.[53] 1 mM Trolox (standard antioxidant) was prepared in MeOH. Working standards were obtained by diluting 1 mM trolox with MeOH. Solutions of known trolox concentration were used for calibration. An ABTS$^{·+}$ radical cation was prepared by passing a 5 mM aqueous stock solution of ABTS (in MeOH) through manganese dioxide powder. Excess manganese dioxide was filtered through a 0.45 µm PTFE filter. Then, 245 µL of ABTS$^{·+}$ solution were added to 5 µL of trolox or to samples and the solutions were stirred for 30 s. The homogenate was shaken vigorously and kept in darkness for 1 h. Absorption of the samples was measured on a UV/VIS Thermo Multiskan Spectrum spectrophotometer at 734 nm and MeOH blanks were run in each assay. Results were expressed as trolox equivalents (µmol trolox / µmol tested compound). Analyses were carried out in triplicate.

4.3.2.4. Antioxidant capacity: DPPH assay

The antioxidant capacity (AC) was also determined through the evaluation of the free radical-scavenging effect on the DPPH

radical.[53] Solutions of known trolox concentration were used for calibration. 5 µL of samples or trolox were mixed with 250 µL of methanolic DPPH (0.025 g L^{-1}). The homogenate was shaken vigorously and kept in darkness for 30 min. Absorption of the samples was measured on the spectrophotometer at 515 nm. Results were expressed as trolox equivalents (µmol trolox / µmol tested compound). Analyses were carried out in triplicate.

4.3.2.5. Analysis of total polyphenols

For the TP assay, each sample was analyzed three times; 20 µL of the samples were mixed with 188 µL of Milli-Q water in a thermo microtiter 96-well plate (nunc^{TM}, Roskilde, Denmark), and 12 µL of F-C reagent and 30 µL of sodium carbonate (200 g/L) were added following a described procedure.[54] The mixtures were incubated for 1 h at room temperature in the dark. After the reaction period, 50 µL of Milli-Q water was added and the absorbance was measured at 765 nm in a UV/Vis Thermo Multiskan Spectrum spectrophotometer (Vantaa, Finland). Results were expressed as mg of gallic acid equivalents (GAE)/g sample.

4.3.3. Aβ42 and tau antiaggregating activities in Escherichia coli cells

4.3.3.1. Cloning and overexpression of Aβ42 peptide

E. coli BL21 (DE3) competent cells were transformed with the pET28a vector (Novagen, Inc., Madison, WI, USA) carrying the DNA sequence of Aβ42. Because of the addition of the initiation codon ATG in front of both genes, the overexpressed peptide contains an additional methionine residue at its N terminus. For overnight culture preparation, lysogeny broth (LB) medium (10 mL) containing kanamycin (50 µg·mL^{-1}) were inoculated with a colony of BL21 (DE3) bearing the plasmid to be expressed at 37 °C. After overnight growth, the OD$_{600}$ was usually 2–2.5. For expression of Aβ42 peptide, overnight culture (20 µL) was transferred into Eppendorf tubes of 1.5 mL containing LB medium (960 µL) with kanamycin (50 µg·mL^{-1}), isopropyl 1-thio-β-D-galactopyranoside (IPTG, 1 mM), 10 µM solution of each hybrid or reference compound in DMSO (10 µL), and 25 µM solution of Th-S in water (10 µL). The samples were grown for 24 h at 37 °C and 1400 rpm using a Thermomixer (Eppendorf, Hamburg, Germany). In the negative control (without drug) the same amount of DMSO was added in the sample.

4.3.3.2. Cloning and overexpression of tau protein

E. coli BL21 (DE3) competent cells were transformed with pTARA containing the RNA-polymerase gene of T7 phage (T7RP) under the control of the promoter pBAD. E. coli BL21 (DE3) with pTARA competent cells were transformed with pRKT42 vector encoding four repeats of tau protein in two inserts. For overnight culture preparation, M9 medium (10 mL) containing glucose (0.5%), ampicillin (50 µg·mL^{-1}), and chloramphenicol (12.5 µg·mL^{-1}) were inoculated with a colony of BL21 (DE3) bearing the plasmids to be expressed at 37 °C. After overnight growth, the OD$_{600}$ was usually 2–2.5. For expression of tau protein, overnight culture (20 µL) was transferred into Eppendorf tubes of 1.5 mL containing M9 medium (970 µL) with arabinose (0.25%), glucose (0.5%), ampicillin (50 µg·mL^{-1}) and chloramphenicol (12.5 µg·mL^{-1}), 10 µM solution of each hybrid or reference compound in DMSO (10 µL), and 25 µM solution of Th-S in water (10 µL). The samples were grown for 24 h at 37 °C and 1400 rpm using a Thermomixer (Eppendorf, Hamburg, Germany). In the negative

control (without drug) the same amount of DMSO was added in the sample.

4.3.3.3. Th-S steady-state fluorescence

Th-S (T1892) and other chemical reagents were purchased from Sigma (St. Louis, MO). Th-S stock solution (2.5 mM) was prepared in double-distilled water purified through a Milli-Q system (Millipore, USA). Fluorescent spectral scans of Th-S were analyzed using an Aminco Bowman Series 2 luminescence spectrophotometer (Aminco-Bowman AB2, SLM Aminco, Rochester, NY, USA). Excitation and emission slit widths of 4 nm were used. Finally, the fluorescence emission at 455 nm, when exciting at 375 nm, was recorded. In order to normalize the Th-S fluorescence as a function of the bacterial concentration, OD$_{600}$ was obtained using a Shimadzu UV-2401 PC UV/Vis spectrophotometer (Shimadzu, Japan). The final fluorescence data were obtained considering as 100% the Th-S fluorescence of the bacterial cells expressing the peptide or protein in the absence of drug and 0% the Th-S fluorescence of the bacterial cells non-expressing the peptide or protein. Final data are the average of ten independent experiments.

4.3.3.4. Optical fluorescence microscopy

Bacterial cells overexpressing Aβ42 peptide and tau protein were incubated for 1 h in the presence of 125 µM Th-S. Th-S was removed by centrifugation and the cells were re-suspended in PBS and placed on a microscope slide. Th-S fluorescence was detected under UV light using a GFP filter with an excitation filter BP480/40 and an emission filter BP527/30 using a Leitz DMIRB microscope. The fluorescence enhancement as a consequence of Th-S binding to IBs has been determined using Quantity One 1-D Analysis Software Version 4.6.9 (Bio-Rad, Hercules, CA, USA) as image processing program.

4.3.4. Determination of brain permeability: PAMPA-BBB assay

The in vitro permeability (P_e) of the novel hybrids and fourteen known drugs through lipid extract of porcine brain membrane was determined by using a parallel artificial membrane permeation assay,[46] using a mixture PBS:EtOH 70:30. Assay validation was made by comparison of the experimental P_e values of the known drugs with their reported values, which showed a good correlation: P_e (exp) = 1.5605 P_e (lit) – 1.0507 (R^2 = 0.9308). From this equation and the limits established by Di et al. for BBB permeation,[46] three ranges of permeability were established: compounds of high BBB permeation (CNS+): P_e (10^{-6} cm s^{-1}) > 5.19; compounds of low BBB permeation (CNS–): P_e (10^{-6} cm s^{-1}) < 2.07; and compounds of uncertain BBB permeation (CNS+/–): 5.19 > P_e (10^{-6} cm s^{-1}) > 2.07.

Table 2
Reported and experimental permeability values (P_e 10^{-6} cm s^{-1}) of 14 commercial drugs used for the PAMPA-BBB assay validation

Compound	Literature value[a]	Experimental value[b]
Cimetidine	0.0	0.70 ± 0.03
Lomefloxacin	1.1	0.75 ± 0.02
Norfloxacin	0.1	0.90 ± 0.02
Ofloxacin	0.8	0.98 ± 0.02
Hydrocortisone	1.9	1.40 ± 0.05
Piroxicam	2.5	1.83 ± 0.19
Clonidine	5.3	6.50 ± 0.05
Corticosterone	5.1	6.70 ± 0.10

Imipramine	13	12.3 ± 0.10
Promazine	8.8	13.8 ± 0.30
Progesterone	9.3	16.8 ± 0.30
Desipramine	12	17.8 ± 0.10
Testosterone	17	24.3 ± 0.46
Verapamil	16	25.2 ± 1.07

[a] Taken from ref. 46.

[b] Values are expressed as the mean ± SD of three independent experiments.

Acknowledgments

References and notes

1. Hardy, J.; Bogdanovic, N.; Winblad, B.; Portelius, E.; Andreasen, N.; Cedazo-Minguez, A.; Zetterberg, H. *J. Int. Med.* **2014**, *275*, 296.
2. Hardy, J.; Selkoe, D. J. *Science* **2002**, *297*, 353.
3. Boutanjangout, A.; Wisniewski, T. *Gerontology* **2014**, in press, DOI: 10.1159/000358875.
4. Castellani, R. J; Zhu, X.; Lee, H.-G.; Moreira, P. I.; Perry, G.; Smith, M. A. *Expert Rev. Neurother.* **2007**, *7*, 473.
5. Sutherland, G. T.; Chami, B.; Youssef, P.; Witting, P. K. *Redox Report* **2013**, *18*, 134.
6. Teixeira, J.; Silva, T.; Andrade, P. B.; F. Borges, F. *Curr. Med. Chem.* **2013**, *20*, 2939.
7. Chakrabarti, S.; Sinha, M.; Thakurta, I. G.; Banerjee, P.; Chattopadhyay, M. *Curr. Med. Chem.* **2013**, *20*, 4648.
8. Rosini, M.; Simoni, E.; Milelli, A.; Minarini, A.; Melchiorre, C. *J. Med. Chem.* **2014**, *57*, 2821.
9. Firuzi, O.; Miri, R.; Tavakkoli, M.; Saso, L. *Curr. Med. Chem.* **2011**, *18*, 3871.
10. Pimplikar, S. W. *Int. J. Biochem. Cell Biol.* **2009**, *41*, 1261.
11. López-Iglesias, B.; Pérez, C.; Morales-García, J. A.; Alonso-Gil, S.; Pérez-Castillo, A.; Romero, A.; López, M. G.; Villarroya, M.; Conde, S.; Rodríguez-Franco, M. I. *J. Med. Chem.* **2014**, *57*, 3773.
12. Belluti, F.; De Simone, A.; Tarozzi, A.; Bartolini, M.; Djemil, A.; A. Bisi, A.; Gobbi, S.; Montanari, S.; Cavalli, A.; Andrisano, V.; Bottegoni, G.; Rampa, A. *Eur. J. Med. Chem.* **2014**, *78*, 157.
13. Thiratmatrakul, S.; Yenjai, C.; Waiwut, P.; Vajragupta, O.; Reubroycharoen, P.; Tohda, M.; Boonyarat, C. *Eur. J. Med. Chem.* **2014**, *75*, 21.
14. Kálai, T.; Altman, R.; Maezawa, I.; Balog, M.; Morisseau, C.; Petrlova, J.; Hammock, B. D.; Jin, L.-W.; Trudell, J. R.; Voss, J. C.; Hideg, K. *Eur. J. Med. Chem.* **2014**, *77*, 343.
15. Qiang, X.; Sang, Z.; Yuan, W.; Li, Y.; Liu, Q.; Bai, P.; Shi, Y.; Ang, W.; Tan, Z.; Deng, Y. *Eur. J. Med. Chem.* **2014**, *76*, 314.
16. Pudlo, M.; Luzet, V.; Ismaïli, L.; Tomassoli, I.; Iutzeler, A.; Refouvelet, B. *Bioorg. Med. Chem.* **2014**, *22*, 2496.
17. Fang, L.; Kraus, B.; Lehmann, J.; Heilmann, J.; Zhang, Y.; Decker, M. *Bioorg. Med. Chem. Lett.* **2008**, *18*, 2905.
18. Chao, X.; He, X.; Yang, Y.; Zhou, X.; Jin, M.; Liu, S.; Cheng, Z.; Liu, P.; Wang, Y.; Yu, J.; Tan, Y.; Huang, Y.; Qin, J.; Rapposelli, S.; Pi, R. *Bioorg. Med. Chem. Lett.* **2012**, *22*, 6498.
19. Zhang, H.-Y. *Biochem. Biophys. Res. Commun.* **2006**, *351*, 578.
20. Viayna, E.; Sola, I.; Bartolini, M.; De Simone, A.; Tapia-Rojas, C.; Serrano, F. G.; Sabaté, R.; Juárez-Jiménez, J.; Pérez, B.; Luque, F. J.; Andrisano, V.; Clos, M. V.; Inestrosa, N. C.; Muñoz-Torrero, D. *J. Med. Chem.* **2014**, *57*, 2549.
21. Pouplana, S.; Espargaró, A.; Galdeano, C.; Viayna, E.; Sola, I.; Ventura, S.; Muñoz-Torrero, D.; Sabate, R. *Curr. Med. Chem.* **2014**, *21*, 1152.
22. Dugasani, S.; Pichika, M. R.; Nadarajah, V. D.; Balijepalli, M. K.; Tandra, S.; Korlakunta, J. N. *J. Ethnopharmacol.* **2010**, *127*, 515.
23. Li, F.; Nitteranon, V.; Tang, X.; Liang, J.; Zhang, G.; Parkin, K. L.; Hu, Q. *Food Chem.* **2012**, *135*, 332.
24. Bak, M.-J.; Ok, S.; Jun, M.; Jeong, W.-S. *Molecules* **2012**, *17*, 8037.
25. Shim, S.; Kwon, J. *Food Chem. Toxicol.* **2012**, *50*, 1454.
26. Camps, P.; Formosa, X.; Galdeano, C.; Muñoz-Torrero, D.; Ramírez, L.; Gómez, E.; Isambert, N.; Lavilla, R.; Badia, A.; Clos, M. V.; Bartolini, M.; Mancini, F.; Andrisano, V.; Arce, M. P.; Rodríguez-Franco, M. I.; Huertas, O.; Dafni, T.; Luque, F. J. *J. Med. Chem.* **2009**, *52*, 5365.
27. Sussman, J. L.; Harel, M.; Frolow, F.; Oefner, C.; Goldman, A.; Toker, L.; Silman, I. *Science* **1991**, *253*, 872.
28. Dvir, H.; Wong, D. M.; Harel, M.; Barril, X.; Orozco, M.; Luque, F. J.; Muñoz-Torrero, D.; Camps, P.; Rosenberry, T. L.; Silman, I.; Sussman, J. L. *Biochemistry* **2002**, *41*, 2970.
29. Nachon, F.; Carletti, E.; Ronco, C.; Trovaslet, M.; Nicolet, Y.; Jean, L.; Renard, P.-Y. *Biochem. J.* **2013**, *453*, 393.
30. Tumiatti, V.; Milelli, A.; Minarini, A.; Rosini, M.; Bolognesi, M. L.; Micco, M.; Andrisano, V.; Bartolini, M.; Mancini, F.; Recanatini, M.; Cavalli, A.; Melchiorre, C. *J. Med. Chem.* **2008**, *51*, 7308.
31. Piazzi, L.; Rampa, A.; Bisi, A.; Gobbi, S.; Belluti, F.; Cavalli, A.; Bartolini, M.; Andrisano, V.; Valenti, P.; Recanatini, M. *J. Med. Chem.* **2003**, *46*, 2279.
32. Mase, N.; Kitagawa, N.; Takabe, K. *Synlett* **2010**, 93.
33. Ellman, G. L.; Courtney, K. D.; Andres Jr., V.; Featherstone, R. M. *Biochem. Pharmacol.* **1961**, *7*, 88.
34. Galdeano, C.; Viayna, E.; Sola, I.; Formosa, X.; Camps, P.; Badia, A.; Clos, M. V.; Relat, J.; Ratia, M.; Bartolini, M.; Mancini, F.; Andrisano, V.; Salmona, M.; Minguillón, C.; González-Muñoz, G. C.; Rodríguez-Franco, M. I.; Bidon-Chanal, A.; Luque, F. J.; Muñoz-Torrero, D. *J. Med. Chem.* **2012**, *55*, 661.
35. Lane, R. M.; Potkin, S. G.; Enz, A. *Int. J. Neuropsychopharmacol.* **2006**, *9*, 101.
36. Prior, R.; Xianli, W.; Schiach, K. *J. Agric. Food Chem.* **2005**, *53*, 4290.
37. Muñoz-Torrero, D.; Pera, M.; Relat, J.; Ratia, M.; Galdeano, C.; Viayna, E.; Sola, I.; Formosa, X.; Camps, P.; Badia, A.; Clos, M. V. *Neurodegener. Dis.* **2012**, *10*, 96.
38. Viayna, E.; Sabate, R.; Muñoz-Torrero, D. *Curr. Top. Med. Chem.* **2013**, *13*, 1820.
39. Inestrosa, N. C.; Alvarez, A.; Pérez, C. A.; Moreno, R. D.; Vicente, M.; Linker, C.; Casanueva, O. I.; Soto, C.; Garrido, J. *Neuron* **1996**, *16*, 881.
40. Inestrosa, N. C.; Dinamarca, M. C.; Alvarez, A. *FEBS J.* **2008**, *275*, 625.
41. De Ferrari, G. V.; Canales, M. A.; Shin, I.; Weiner, L. M.; Silman, I.; Inestrosa, N. C. *Biochemistry* **2001**, *40*, 10447.
42. Cui, M. *Curr. Med. Chem.* **2014**, *21*, 82.
43. Camps, P.; El Achab, R.; Morral, J.; Muñoz-Torrero, D.; Badia, A.; Baños, J. E.; Vivas, N. M.; Barril, X.; Orozco, M.; Luque, F. J. *J. Med. Chem.* **2000**, *43*, 4657.
44. Hedberg, M. M.; Clos, M. V.; Ratia, M.; Gonzalez, D.; Unger Lithner, C.; Camps, P.; Muñoz-Torrero, D.; Badia, A.; Giménez-Llort, L.; Nordberg, A. *Neurodegener. Dis.* **2010**, *7*, 379.
45. Kroon, P. A.; Clifford, M. N.; Crozier, A.; Day, A. J.; Donovan, J. L.; Manach, C.; Williamson, G. *Am. J. Clin. Nutr.* **2004**, *80*, 15.
46. Di, L.; Kerns, E. H.; Fan, K.; McConnell, O. J.; Carter, G. T. *Eur. J. Med. Chem.* **2003**, *38*, 223.
47. Mattarei, A.; Azzolini, M.; Carraro, M.; Sassi, N.; Zoratti, M.; Paradisi, C.; Biasutto, L. *Mol. Pharmaceutics* **2013**, *10*, 2781.
48. Barnes, S.; Prasain, J.; D'Alessandro, T.; Arabshahi, A.; Botting, N.; Lila, M. A.; Jackson, G.; Janle, E. M.; Weaver, C. M. *Food Funct.* **2011**, *2*, 235.
49. Viayna, E.; Gómez, T.; Galdeano, C.; Ramírez, L.; Ratia, M.; Badia, A.; Clos, M. V.; Verdaguer, E.; Junyent, F.; Camins, A.; Pallàs, M.; Bartolini, M.; Mancini, F.; Andrisano, V.; Arce, M. P.; Rodríguez-Franco, M. I.; Bidon-Chanal, A.; Luque, F. J.; Camps, P.; Muñoz-Torrero, D. *ChemMedChem* **2010**, *5*, 1855.

50. Olsson, M. H. M.; Sondergard, C. R.; Rostkowski, M.; Jensen, J. H. *J. Chem. Theory Comput.* **2011**, *7*, 525.

51. Case, D. A.; Darden, T. A.; Cheatham, T. E., III; Simmerling, C. L.; Wang, J.; Duke, R. E.; Luo, R.; Walker, R. C.; Zhang, W.; Merz, K. M.; Roberts, B.; Hayik, S.; Roitberg, A.; Seabra, G.; Swails, J.; Goetz, A. W.; Kolossváry, I.; Wong, K. F.; Paesani, F.; Vanicek, J.; Wolf, R. M.; Liu, J.; Wu, X.; Brozell, S. R.; Steinbrecher, T.; Gohlke, H.; Cai, Q.; Ye, X.; Wang, J.; Hsieh, M.-J.; Cui, G.; Roe, D. R.; Mathews, D. H.; Seetin, M. G.; Salomon-Ferrer, R.; Sagui, C.; Babin, V.; Luchko, T.; Gusarov, S.; Kovalenko, A.; Kollman, P. A. *AMBER 12*, University of California, San Francisco, **2012**.

52. Ruiz-Carmona, S.; Alvarez-García, D.; Foloppe, N.; Garmendia-Doval, A. B.; Juhos, S.; Schmidtke, P.; Barril, X.; Hubbard, R. E.; Morley, S. D. *PLOS Comput. Biol.* **2014**, *10*, e1003571.

53. Vallverdú-Queralt, A.; Medina-Remón, A.; Casals-Ribes, I.; Amat, M.; Lamuela-Raventós, R. M. *J. Agric. Food Chem.* **2011**, *59*, 11703.

54. Vallverdú-Queralt, A.; Rinaldi de Alvarenga, J. F.; Estruch, R.; Lamuela-Raventos, R. M. *Food Chem.* **2013**, *141*, 3366.